ChemistryOPEN

Supporting Information

Pulsed Magnetic Resonance to Signal-Enhance Metabolites within Seconds by utilizing *para*-Hydrogen

Sergey Korchak,[a, b] Shengjun Yang,[a, b] Salvatore Mamone,[a, b] and Stefan Glöggler*[a, b]

open_201800024_sm_miscellaneous_information.pdf

Supplementary information

1. Materials and instruments

All the chemicals were purchased from commercial suppliers and used as received. Thin-layer chromatography (TLC) analysis was carried out on pre-coated silica plates. Column chromatography was performed using silica gel (200-300 mesh) using eluents in the indicated v/v ratio. ^{1}H NMR and ^{13}C NMR spectra were acquired on a Bruker ultrashield 300 MHz or Bruker 900 MHz spectrometer at 25 °C, respectively. Chemical shifts of the hydrogenation experiments in the main text and SI are given in respect to the solvent used which is acetone-d_6 (2.09 ppm for ^{1}H and 205.87 and 30.60 ppm for ^{13}C). In the SI for characterization purposes, the NMR spectra are recorded in chloroform ($CDCl_3$) if not stated otherwise and chemical shifts (δ) are given in parts per million (ppm) relative to $CHCl_3$ (7.26 ppm for ^{1}H) or $CDCl_3$ (77.0 ppm for ^{13}C). High-resolution mass spectrometry (HR MS-ESI) spectra were taken on Thermo Scientific LTQ Orbitrap XL.

1.1 General synthesis consideration

In order to generate high levels of metabolite polarization we have to first design a molecular system in which para-hydrogen spin order can efficiently be transferred to the metabolite of interest. For this, we introduce a sidearm that is deuterated to prolong longitudinal relaxation times and contains one intermediate ^{13}C species to which polarization is transferred at first. As explained in detail in the main text, the polarization can afterwards be transferred from this ^{13}C nuclei to a ^{13}C nuclei in a metabolite of interest. The sidearm, 3-phenyl(1-^{13}C,$^{2}H_2$)prop-2-yn-1-ol, attached to a ^{13}C labeled metabolite via the carboxylic acid is synthesized as follows (see Figure S1): phenylacetylene is reacted with deuterated and ^{13}C enriched formaldehyde to obtain the sidearm. Isotopically enriched formaldehyde is mostly commercially available in D_2O. However, the presence of water is undesirable for the coupling reaction with phenylacetylene and extracting the labeled formaldehyde as a gas is difficult. We therefore utilized the approach to convert ^{13}C and ^{2}H enriched methyl iodide with trimethylamine N-oxide (TMAO) in THF into formaldehyde.[1] After 1 hour of reaction at 70°C the methyl iodide had completely transformed into formaldehyde and its oligomer (due to the high conversion starting from labeled methyl iodide was considerable less expensive than utilizing formaldehyde as a starting material). Without purification, we reacted the obtained slurry with phenylacetylene under inert gas atmosphere to yield the sidearm. We utilized the labeled sidearm afterwards in esterification reactions with acetate and pyruvate to obtain the reactant for the para-hydrogen experiment. We would like to note that we designed the alkyne precursor with a non-terminal alkyne moiety. This has the advantage that a hydrogenation catalyst can be utilized to selectively yield the alkene (double bond).[2]

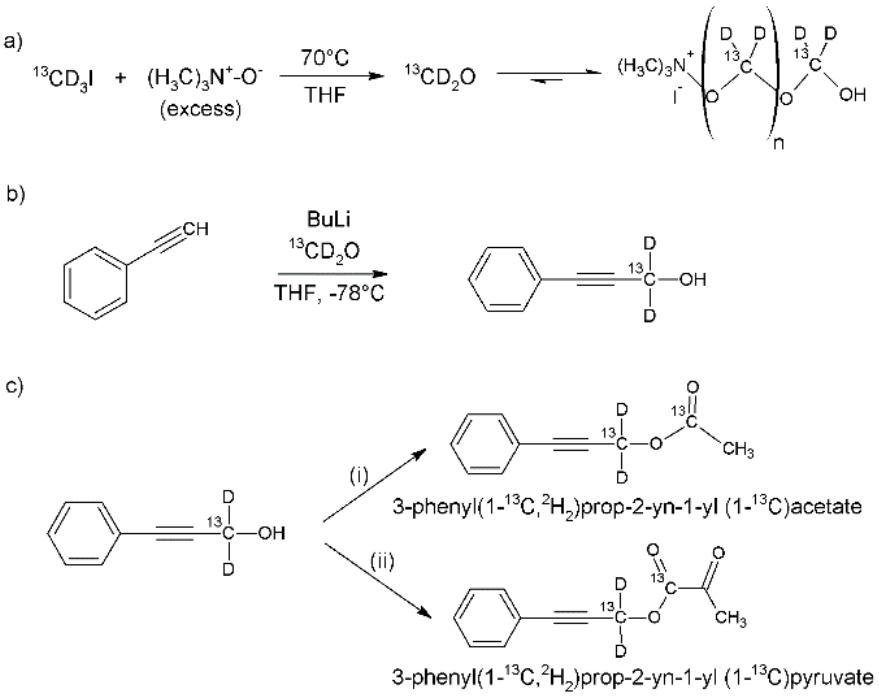

Figure S1. Synthesis of the metabolite derivatives. a) Reaction of labeled methyl iodide into formaldehyde and its oligomer. b) Synthesis of the sidearm. c) Esterification of the sidearm with acetate or pyruvate. We used the following reaction conditions: (i) Acetic anhydride-1,1′-$^{13}C_2$, DMAP, Et_3N, anhydrous dichloromethane, N_2, rt (ii) Pyruvic-1-^{13}C acid, Dean-stark, anhydrous benzene, p-TsOH, 92 °C

1.2 Synthesis of ^{13}C-formaldehyde-d$_2$ ($^{13}CD_2O$)[1]:

To a solution of trimethylamine *N*-oxide (375 mg, 5 mmol) in anhydrous THF (12.0 mL) at 70 °C, ^{13}C-Iodomethane-d$_3$ ($^{13}CD_3I$) (62.5 uL, 1 mmol) was added. Upon addition of iodomethane, white precipitate was immediately found at the bottom of the flask. After stirring for 1 hour, the suspension was cooled down to room temperature and used for the next reaction immediately without further purification.

1.3 Synthesis of 3-Phenyl-2-propyn-1,1-d$_2$-1-ol-1-^{13}C

To a solution of phenylacetylene (100 mg) in anhydrous THF, n-butyl lithium (0.8 mL, 1.6 M in hexane) was dropwise added at -78 °C under N_2 atmosphere. A solution of ^{13}C-formaldehyde-d$_2$ in THF was added after 45 min and then stirred for another 1 hour. After stirring overnight at room temperature, the reaction was quenched by addition of saturated NH_4Cl solution (25 mL) and extracted with diethyl ether (20 mL× 3), the organic layers combined and dried over Na_2SO_4. After filtration, the volatile was evaporated under reduced pressure and the crude product was purified by column chromatography on silica gel (Eluent: petroleum ether : ethyl acetate = 8 : 1 to 4 : 1) to give an oil (42 mg, 31%).

^{1}H NMR (300 MHz, $CDCl_3$): δ 7.46-7.42 (m, 2 H), 7.33-7.30 (m, 3 H).

^{13}C {^{1}H} NMR (75 MHz, $CDCl_3$) : δ 131.66, 128.47, 128.28, 122.49 (d, ^{13}C–^{13}C, $^3J_{C,C}$ = 1.60 Hz), 87.11 (d, ^{13}C–^{13}C, $^1J_{C,C}$ = 73.60 Hz), 85.64 (d, ^{13}C–^{13}C, $^2J_{C,C}$ = 12.40 Hz), 51.10 (quint, ^{13}C–^2D, $^1J_{C,D}$ = 22.60 Hz).

HR MS (ESI): m/z calcd for $C_8{}^{13}CH_6D_2ONa^+$ [M + Na^+] 158.0626, found 158.0627.

1.4 Synthesis of 3-Phenyl-2-propyn-1-^{13}C-1,1-d_2-1-yl 1-^{13}C-acetate

Into an oven dried 50 mL round-bottom flask, 3-Phenyl-2-propyn-1,1-d_2-1-ol-1-^{13}C (110 mg), DMAP (50 mg), Acetic anhydride-1,1′-$^{13}C_2$ (214 uL) and Et_3N (286 uL) were added in turn under N_2 atmosphere and dissolved in anhydrous dichloromethane (3 mL). The resulting solution was stirred at room temperature overnight. After the addition of saturated NH_4Cl solution (20 mL), the reaction solution was extracted with diethyl ether (20 mL× 3), the organic layers combined and dried over Na_2SO_4. After filtration, the solution was concentrated under reduced pressure. The crude product was purified by column chromatography on silica gel (Eluent: petroleum ether : ethyl acetate = 10 : 1 to 5 : 1) to give an oil (93 mg, 64%).

^{1}H NMR (300 MHz, $CDCl_3$): δ 7.47-7.43 (m, 2 H), 7.34-7.30 (m, 3 H), 2.14-2.12 (dd, 3 H, ^{1}H–^{13}C, $^2J_{C,H}$ = 6.80 Hz, $^4J_{C,H}$ = 0.8 Hz).

^{13}C {^{1}H} NMR (225 MHz, $CDCl_3$) : δ 170.19 (d, ^{13}C–^{13}C, $^2J_{C,C}$ = 2.30 Hz), 131.79, 128.67, 128.20, 122.03 (d, ^{13}C–^{13}C, $^3J_{C,C}$ = 1.60 Hz), 86.30 (d, ^{13}C–^{13}C, $^2J_{C,C}$ = 13.70 Hz), 82.78 (d, ^{13}C–^{13}C, $^1J_{C,C}$ = 79.60 Hz), 52.25 (quint-d, ^{13}C–^{2}D, $^1J_{C,D}$ = 23.30 Hz, ^{13}C–^{13}C, $^2J_{C,C}$ = 2.30 Hz), 20.67 (dd, ^{13}C–^{13}C, $^1J_{C,C}$ = 59.40 Hz).

HR MS (ESI): m/z calcd for $C_9{}^{13}C_2H_8D_2O_2Na^+$ [M + Na^+] 201.0766, found 201.0764.

1.5 Synthesis of 3-Phenyl-2-propyn-1-^{13}C-1,1-d_2-1-yl 1-^{13}C-pyruvate

Into a 50-mL round bottom flask equipped with a dean-stark apparatus, 3-Phenyl-2-propyn-1, 1-d_2-1-ol-1-^{13}C (145 mg), pyruvic-1-^{13}C acid (95 mg) and *p*-TsOH (15 mg) were added under N_2 atmosphere. Benzene (16 mL) was added to dissolve the mixture and subsequently heated to 92 °C for 12 hours. After cooling down the solution to room temperature, saturated $NaHCO_3$ solution was added and then extracted by diethyl ether (20 mL× 3), the organic layers were dried over Na_2SO_4. The volatile was concentrated under reduced pressure after filtration. The residue was purified by flash column chromatography on silica gel (Eluent: petroleum ether : ethyl acetate = 10 :1) to give an oil (75 mg, 34%).

^{1}H NMR (300 MHz, $CDCl_3$): δ 7.46-7.45 (m, 2 H), 7.35-7.31 (m, 3 H), 2.52 (d, 3 H, ^{1}H–^{13}C, *J* = 1.60 Hz).

^{13}C {^{1}H} NMR (225 MHz, $CDCl_3$) : δ 190.10 (dd, ^{13}C–^{13}C, $^1J_{C,C}$ = 67.10 Hz, ^{13}C–^{13}C, $^3J_{C,C}$ = 1.30 Hz), 159.91 (d, ^{13}C–^{13}C, $^2J_{C,C}$ = 2.51 Hz), 131.94, 129.04, 128.34, 121.71 (d, ^{13}C–^{13}C, $^3J_{C,C}$ = 1.60 Hz), 87.63 (d, ^{13}C–^{13}C, $^2J_{C,C}$ = 14.0 Hz), 81.29 (d, ^{13}C–^{13}C, $^1J_{C,C}$ = 80.40 Hz), 54.10 (quint-d, ^{13}C–^{2}D, $^1J_{C,D}$ = 23.50 Hz, ^{13}C–^{13}C, $^2J_{C,C}$ = 2.51 Hz), 20.81 (d, ^{13}C–^{13}C, $^2J_{C,C}$= 16.80 Hz). **HR MS** (ESI): m/z calcd for $C_{10}{}^{13}C_2H_8D_2O_3Na^+$ [M + Na^+] 229.0715, found 229.0715.

1.6 Characterization of the sidearm molecules:

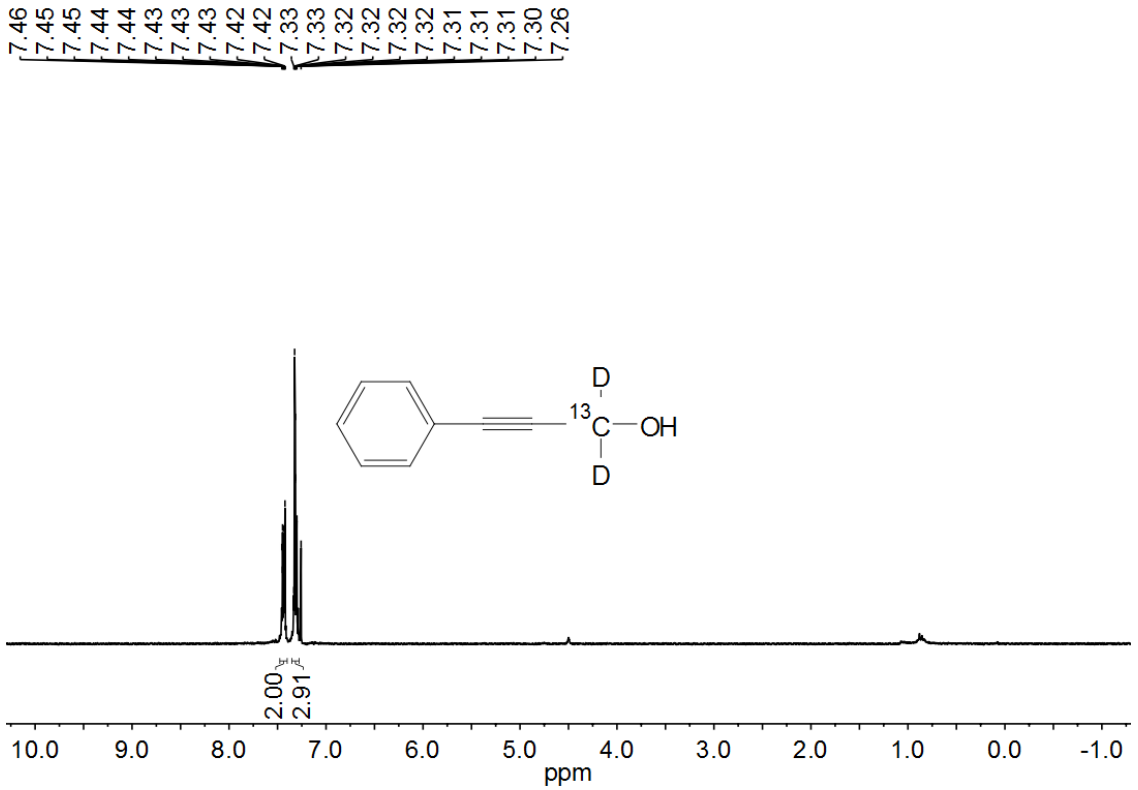

Figure S2. ^{1}H NMR spectrum of 3-Phenyl-2-propyn-1,1-d$_2$-1-ol-1-^{13}C recorded on a Bruker 300 MHz spectrometer in CDCl$_3$.

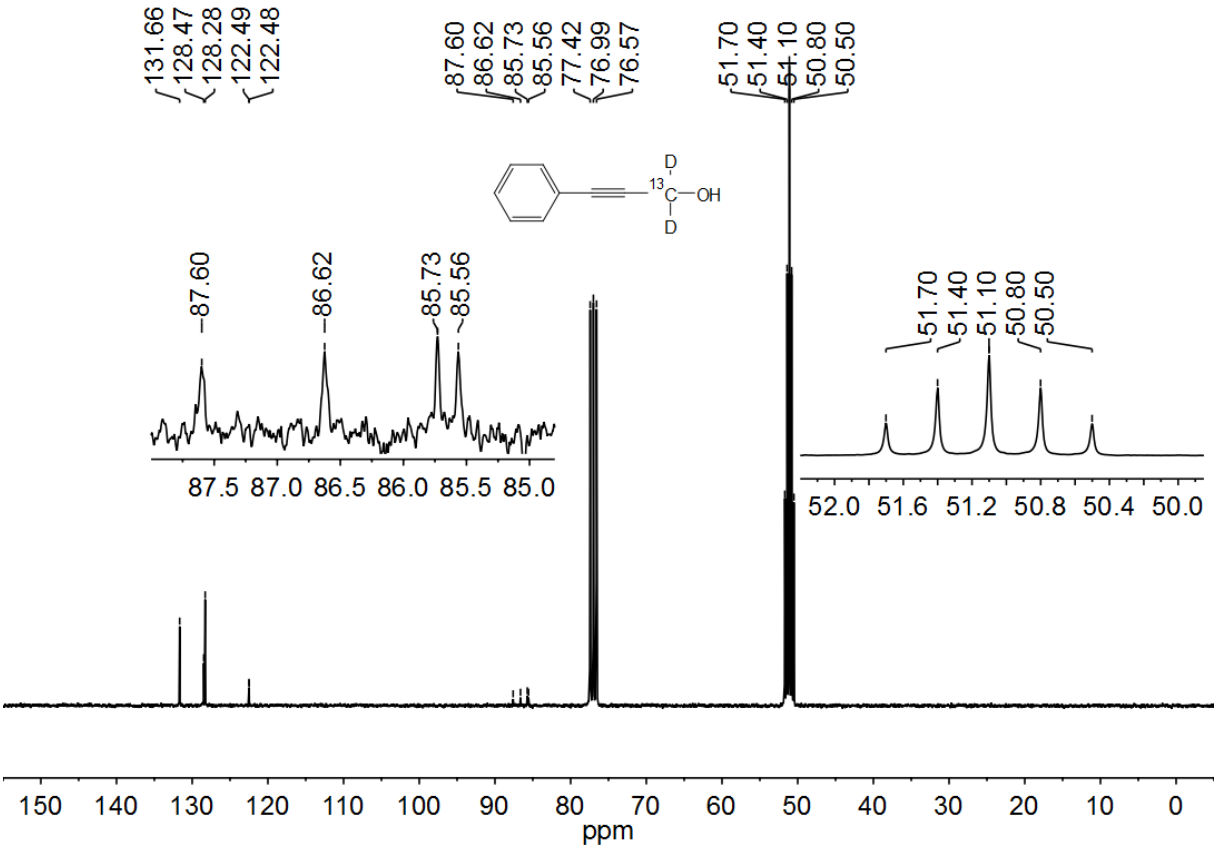

Figure S3. ^{13}C NMR spectrum of 3-Phenyl-2-propyn-1,1-d$_2$-1-ol-1-^{13}C recorded on a Bruker 300 MHz spectrometer in CDCl$_3$.

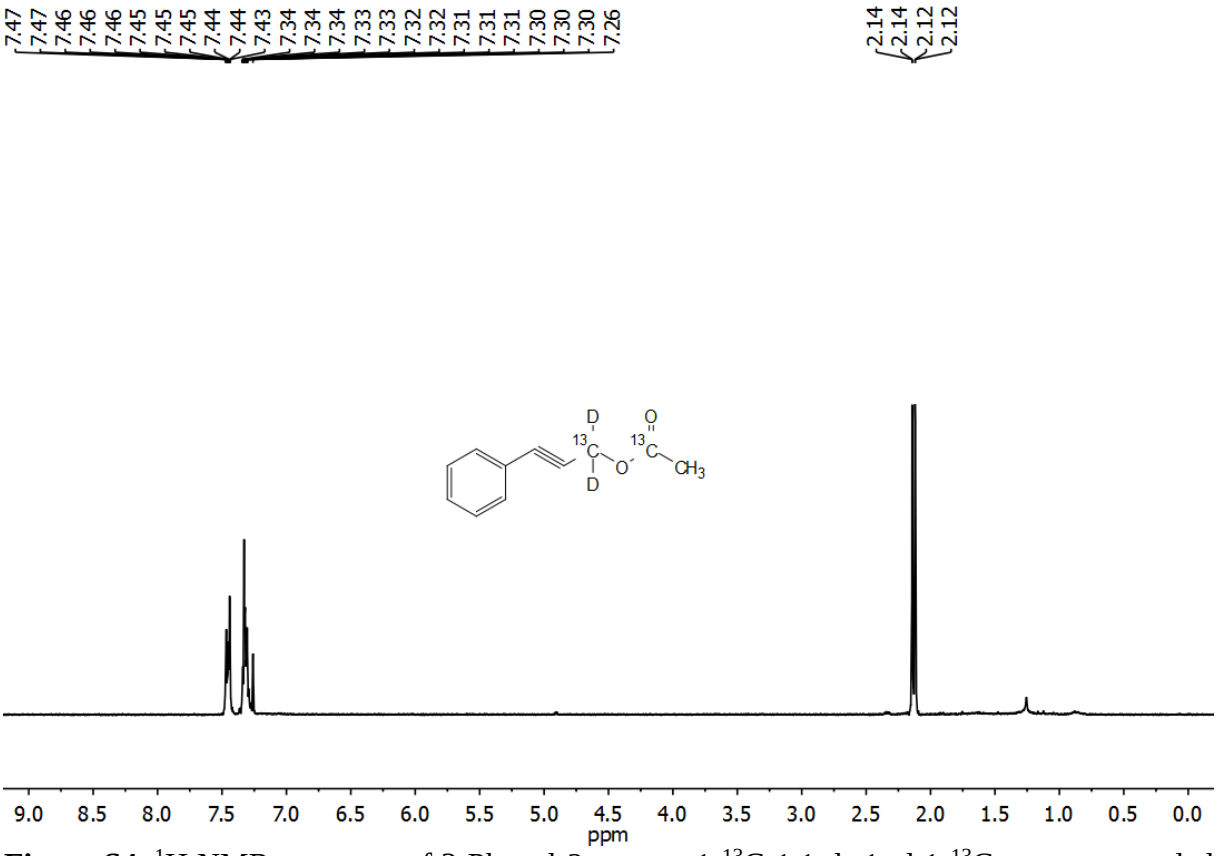

Figure S4. ^{1}H NMR spectrum of 3-Phenyl-2-propyn-1-^{13}C-1,1-d$_2$-1-yl 1-^{13}C-acetate recorded on a 300 MHz spectrometer in $CDCl_3$.

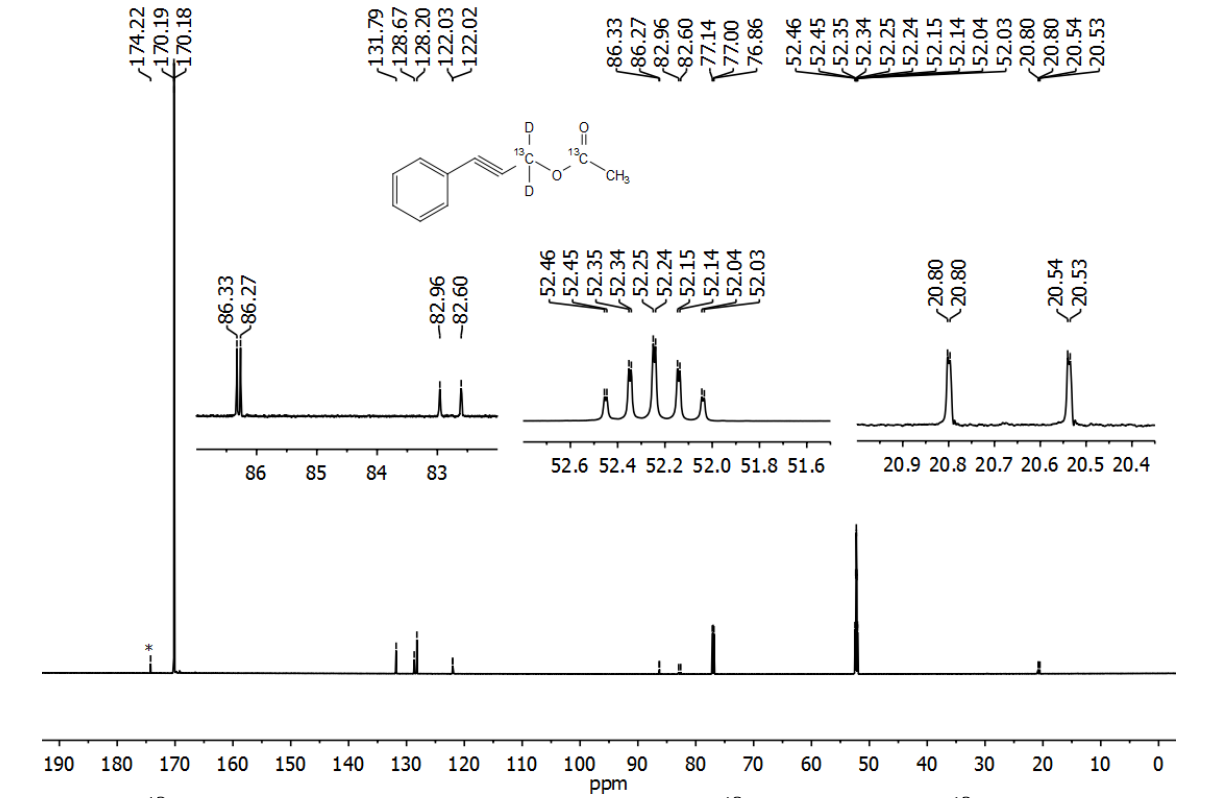

Figure S5.^{13}C NMR spectrum of 3-Phenyl-2-propyn-1-^{13}C-1,1-d$_2$-1-yl 1-^{13}C-acetate recorded on a Bruker 900 MHz spectrometer in $CDCl_3$. "*" denotes the signal of free acetic acid.

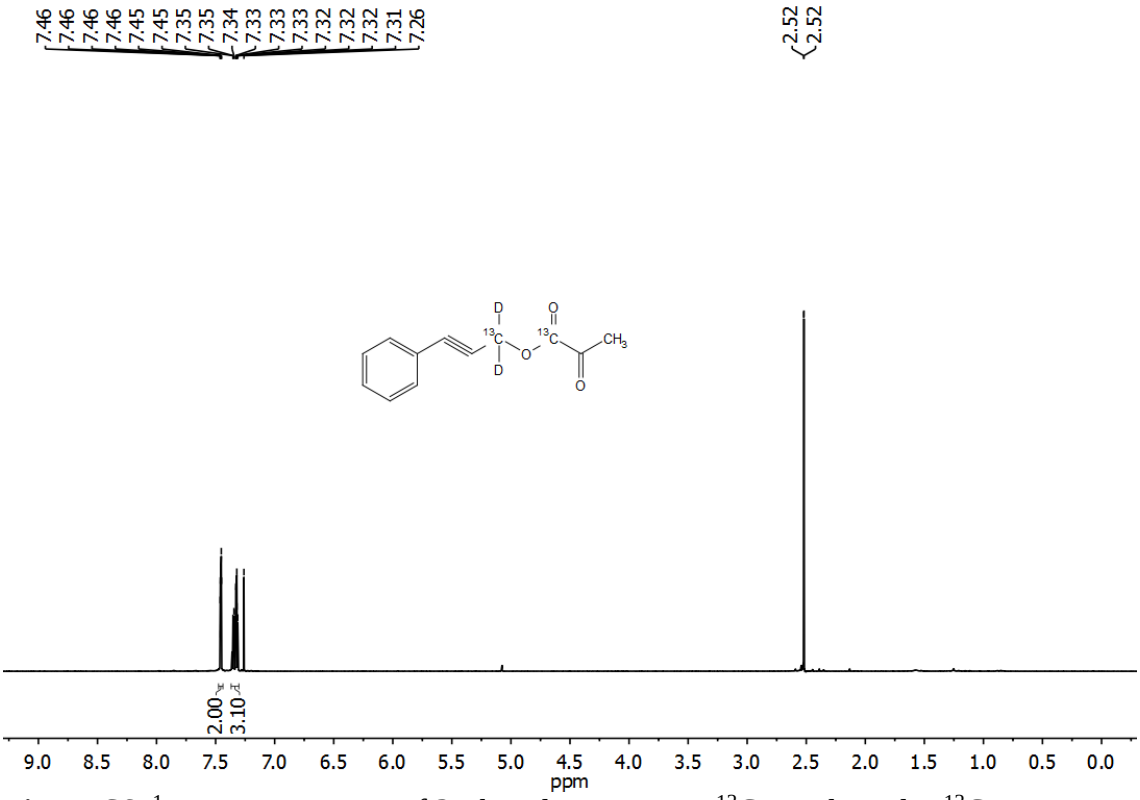

Figure S6. ^{1}H NMR spectrum of 3-Phenyl-2-propyn-1-^{13}C-1,1-d$_2$-1-yl 1-^{13}C-pyruvate recorded on a Bruker 300 MHz spectrometer in $CDCl_3$.

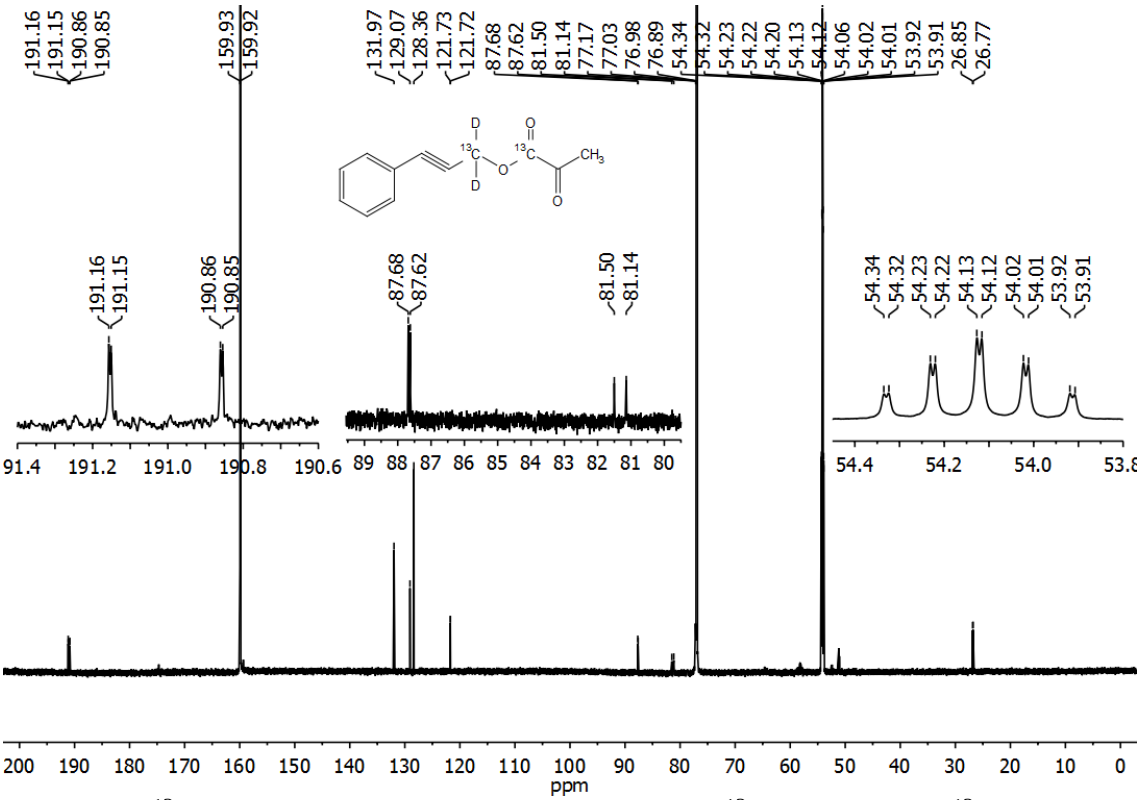

Figure S7. ^{13}C NMR spectrum of 3-Phenyl-2-propyn-1-^{13}C-1,1-d$_2$-1-yl 1-^{13}C-pyruvate recorded on a Bruker 900 MHz spectrometer in $CDCl_3$.

1.7 NMR experiments

Stock solutions of the synthetized precursors were prepared and their concentrations were calibrated with respect to an external standard sample with known concentration (50 mM 3,4,5-trichloropyridine). By dilution of the stock solutions in acetone-d_6 the 1.5 mM precursor samples were achieved and after addition of 5 mM commercially available catalyst ([1,4-Bis(diphenylphosphino)butane](1,5-cyclooctadiene)rhodium(I) tetrafluoroborate) were placed in 5 mm NMR tube. Para-enriched hydrogen gas was obtained using a Bruker Para-Hydrogen Generator (BPHG 90). The nominal conversion temperature in the generator was set to 36 K providing 92% para-enriched hydrogen gas. Gaseous para-hydrogen was delivered through a capillary and bubbled through the solution at 320K using a home-built automated setup. The gas delivery setup follows the idea of Ref. [3] The para-hydrogen gas was kept at 6 bar to achieve higher concentration of the dissolved gas and increase the rate of the hydrogenation reaction. The NMR measurements were done in a standard double resonance inverse probehead in a 7 T cryomagnet coupled to a Bruker Spectrometer System (Avance III HD, 300 MHz). Following a bubbling period of 20 s and a settling time of 2 s, an NMR pulse sequence was initiated to transfer para-hydrogen spin order to observable magnetization and the FID of the enhanced ^{1}H or ^{13}C signal was recorded. The thermal spectrum of a 80-fold concentrated reference was recorded after a 90° excitation pulse (10 scans with an interscan delay of 240 s) for signal enhancement calculations with the polarized spectra. The hyperpolarized spectra were recorded in a single scan applying the ESOTHERIC sequence for spin order transfer following the para-hydrogenation procedure. The cleaved spectra were recorded after 0.2 ml of basic 0.5 M NaOD in 50%/50% v/v D_2O/methanol-d_4 solution was added to a 0.2 ml solution in acetone of the cinnamyl esters to release acetate or pyruvate.

The spin-lattice relaxation time $T_1(H_2)$ of the cis-protons in the *cis*-cinnamyl ester was measured in a standard non-selective inversion-recovery delay-acquire experiment. The singlet lifetime $T_s(H_2)$ was measured by using a 4-scan APSOC sequence with a variable delay between the magnetization-to-singlet (M2S) conversion block and singlet-to-magnetization reconversion block (S2M).[4] For the M2S and S2M blocks, linearly increasing and decreasing ramps, with the maximum RF-field B_1 corresponding to a nutation frequency of ν_1=2 KHz, were used. The duration of each block was 150 ms. The shift in the offset in the APSOC scans was Δ=50 Hz. [4]

1.8 Detailed discussion of the ESOTHERIC sequence

In this section a step by step analysis of the ESOTHERIC sequence, with reference to Figure 3 in the main text, is given. The analysis is based on the product operator formalism for spin ½.[2] In the following discussion, all the couplings are assumed positive for sake of simplicity. A change in the sign in any of the couplings affects only the relative sign of the intermediate and final spin density operators. All pulses are assumed to be ideal (i.e. instantaneous with perfect nutation angle and phase) and relaxation effects are disregarded. The high magnetic field condition is used to truncate the homonuclear *J*-coupling Hamiltonians to $H_{12}=2\pi J_{12}I_{1z}I_{2z}$ and $H_{34}=2\pi J_{12}S_{3z}S_{4z}$ when the couplings J_{12} and J_{34} are much smaller than the chemical shift difference δ_{12} and δ_{34}, i.e. $2\pi J_{12}/(\delta_{12}B_0)<<1$ and $2\pi J_{34}/(\delta_{34}B_0)<<1$.

Following para-hydrogenation, it is possible to prove that the spin density operator at the beginning of the sequence is $\rho_0=I_{1z}I_{2z}$. A non-selective $90°_y$ pulse on the ^{1}H channel convert longitudinal 2-spin order $\rho_0=I_{1z}I_{2z}$ into transverse 2-spin order $\rho_1=I_{1x}I_{2x}$ on protons. In section A of the pulse sequence, the evolution of transverse spin order is determined only by the heteronuclear ^{1}H-^{13}C *J*-coupling due to the simultaneous 180° pulses on these two channels.

After the time interval $\Delta_A=1/(2J_{13})$ the density matrix becomes $\rho_2=2I_{1y}I_{2x}S_{3z}$. The following $90°_y$ pulse on ^1H creates anti-phase magnetization on the two protons so that $\rho_3=2I_{1y}I_{2z}S_{3z}$ which evolves into $\rho_4=-I_{1x}S_{3z}$ after a period $\Delta_B=1/(2J_{12})$ under the influence of the homonuclear proton scalar coupling J_{12}. All the heteronuclear J_{HX} couplings as well as chemical shifts are ineffective during the evolution period Δ_B. The next simultaneous ^1H-^{13}C 90_y pulses exchange the role of longitudinal and transverse magnetization between spin 2 and 3 so that $\rho_5=I_{1z}S_{3x}$.

Figure 3b$_1$) in the main text shows the pulse sequence to complete the transfer to the first carbon $^{13}C_3$, starting from the time point 5. In virtue of the simultaneous 180° pulses on the ^1H and ^{13}C channels, the evolution of the spin density operator during the block C_1 is determined by the heteronuclear $^1H_1$-$^{13}C_3$ J-coupling when the pulse on the ^{13}C channel act selectively on $^{13}C_3$. Indeed, the truncated homonuclear J_{HH}-coupling Hamiltonian commutes with ρ_5 and plays no role in its evolution. The $^{13}C_3$ 180° pulse refocuses the $^{13}C_3$-D J-coupling and $^{13}C_3$ chemical shifts as well as the homonuclear $^{13}C_3$-$^{13}C_4$ J-coupling. It follows that $\rho_5=I_{1z}S_{3x}$ evolves into $\rho_6=S_{3y}/2$ over a period $\Delta_{C1}=1/(2J_{13})$. If the last 180° flip-pulse on the carbon channels is non-selective the homonuclear $^{13}C_3$-$^{13}C_4$ J-coupling is not refocused and $\rho_6=S_{3y}/2\cos[\pi J_{34}/(2J_{13})]- S_{3y}S_{4z}\sin[\pi J_{34}/(2J_{13})]$. The antiphase term is negligible when $J_{34}/J_{12}<<1$.

Figure 3b$_2$) shows the pulse sequence to complete the transfer to carbon $^{13}C_4$, starting from the time point 5. As above, evolution under the proton-carbon coupling J_{13} is allowed for a period $\Delta_{C1}=1/(2J_{13})$ to bring the density matrix to in-phase magnetization on the methylene carbon. All proton-carbon couplings are then switched off by a decoupling sequence acting on the proton channel only. During the time Δ_{C1} and for all the duration of block C, the homonuclear $^{13}C_3$-$^{13}C_4$ direct coupling brings the density operator into $\rho_6=(S_{3y}/2)\times\cos(\pi J_{34}\Delta_{C1}) - S_{3x}S_{4z}\times\sin(\pi J_{34}\Delta_{C1})$ and then fully convert it into $\rho_7=-S_{3x}S_{4z}$ over the full period $\Delta_C=1/(2J_{34})$. The $90°_y$ pulse exchanges the role of spin 3 and 4 in the anti-phase carbon magnetization so that $\rho_8=S_{3z}S_{4x}$. After the evolution period $\Delta_D=1/(2J_{34})$ the density operator becomes $\rho_9=S_{4y}/2$. Notably, the effects of carbon chemical shifts as well as deuterium scalar couplings can be discarded in virtue of the 180° pulse in the middle of the blocks C and D.

The presence of finite J-couplings other than those considered above reduces the efficiency of the transfer from proton longitudinal spin order to in phase magnetization on the hetero-nuclei. When considering the effect of the heteronuclear coupling J_{23}, and neglecting J_{14} and J_{24}, the complete product operator analysis shows that the efficiency for transfer from $I_{1z}I_{2z}$ to $S_{3y}/2$ (and then to $S_{4y}/2$) is

$$\phi=\{[\cos(\pi J_{13}\Delta)]^2\,[\sin(\pi J_{23}\Delta)]^2+[\cos(\pi J_{23}\Delta)]^2\,[\sin(\pi J_{13}\Delta)]^2\}\,\sin(\pi J_{12}\Delta_B)$$

The efficiency does not depend on the sign of the heteronuclear couplings J_{13} and J_{23}. The formula indicates that the maximum efficiency is reached for $\Delta_B=1/(2|J_{12}|)$. For fixed J_{13} and J_{23}, the numerical maximization of the efficiency ϕ and of the delay $\Delta=\Delta_A=\Delta_{C1}$ is shown in figure S8. For $|J_{23}|<<|J_{13}|$ the transfer is close to 1 with $\Delta_M=1/(2|J_{13}|)$. For $|J_{23}|=|J_{13}|$ the transfer is 0.5 with $\Delta_M=1/(4|J_{13}|)$. In general the transfer efficiency is larger than 0.5 for an optimal Δ_M slightly larger than $1/[2(|J_{13}|+|J_{23}|)]$. As shown in the contour plot in figure S9, the sequence

behaves favorably with respect to missets in the timing Δ. Indeed, the efficiency remains within 5% of the maximum achievable ϕ_M for deviations of Δ within ±10% of the optimal value Δ_M.

Finally, the action of the heteronuclear-couplings J_{24}, J_{34} reduces the efficiency transfer by a factor $\cos[\pi J_{14}\Delta_A]\times\cos[\pi J_{24}\Delta_A]$ since the couplings to the hetero-nucleus 4 are relevant only in the section A of the sequence.

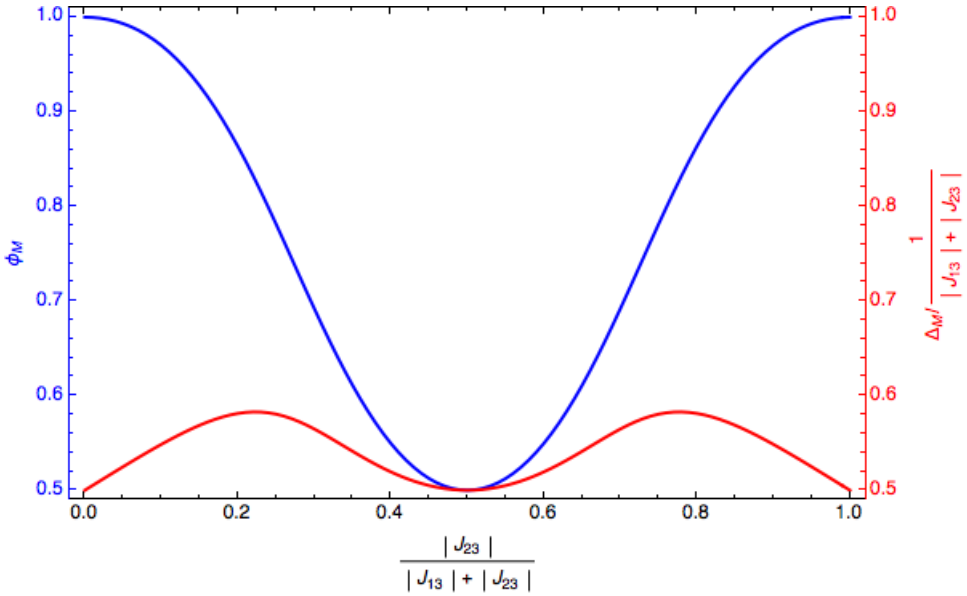

Figure S8. The plot shows the maximum efficiency of transfer ϕ_M, in blue with scale on the left side, as obtained for the optimal timing Δ_M, in red with scale on the right side, in function of the adimensional ratio of $|J_{23}|/(|J_{13}|+|J_{23}|)$.

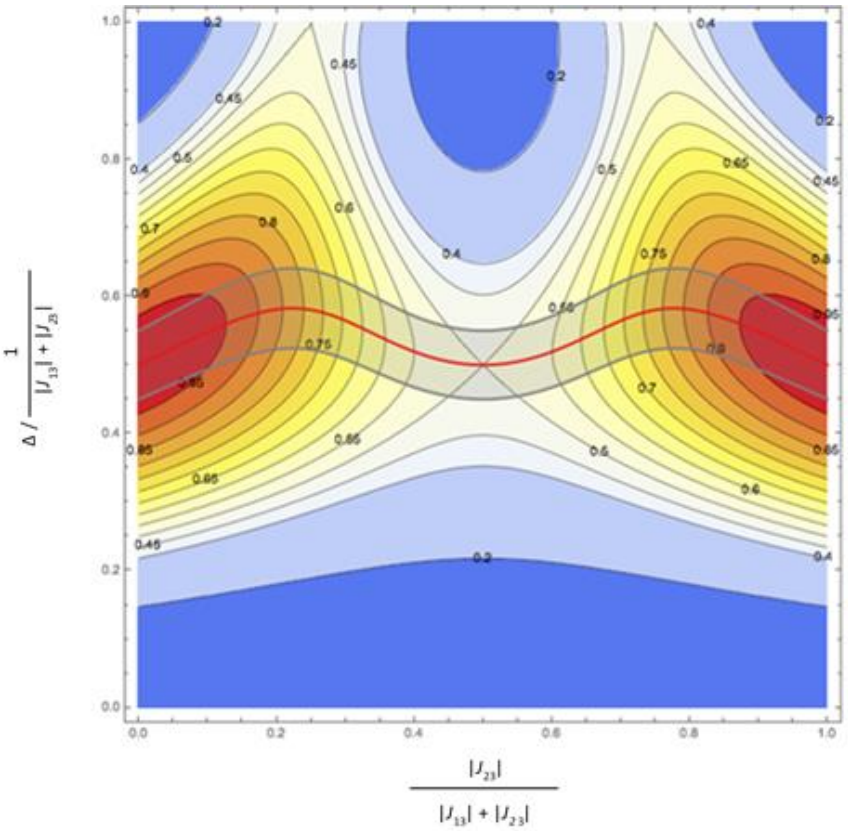

Figure S9. The contour plot shows the efficiency of transfer ϕ as function of the adimensional ratio of $|J_{23}|/(|J_{13}|+|J_{23}|)$ and as function of Δ. The red line represents the optimal timing Δ_M as function of $|J_{23}|/(|J_{13}|+|J_{23}|)$. The shadowed region within the grey lines represents deviations of Δ within ±10% of the optimal value Δ_M.

1.9 Spectra relative to the intermediate spin order transfer

All the samples were dissolved in acetone-d_6 at the concentrations indicated in the accompanying caption. In the samples subjected to para-hydrogentation, the concentration of the catalyst Bis(diphenylphosphino)butane](1,5-cyclooctadiene)rhodium(I) tetrafluoroborate was 5mM. The samples were placed in standard 5mm NMR tubes and spectra were recorded at 320 K in a 7 T cryomagnet after the pulse sequence specified in the respective caption.

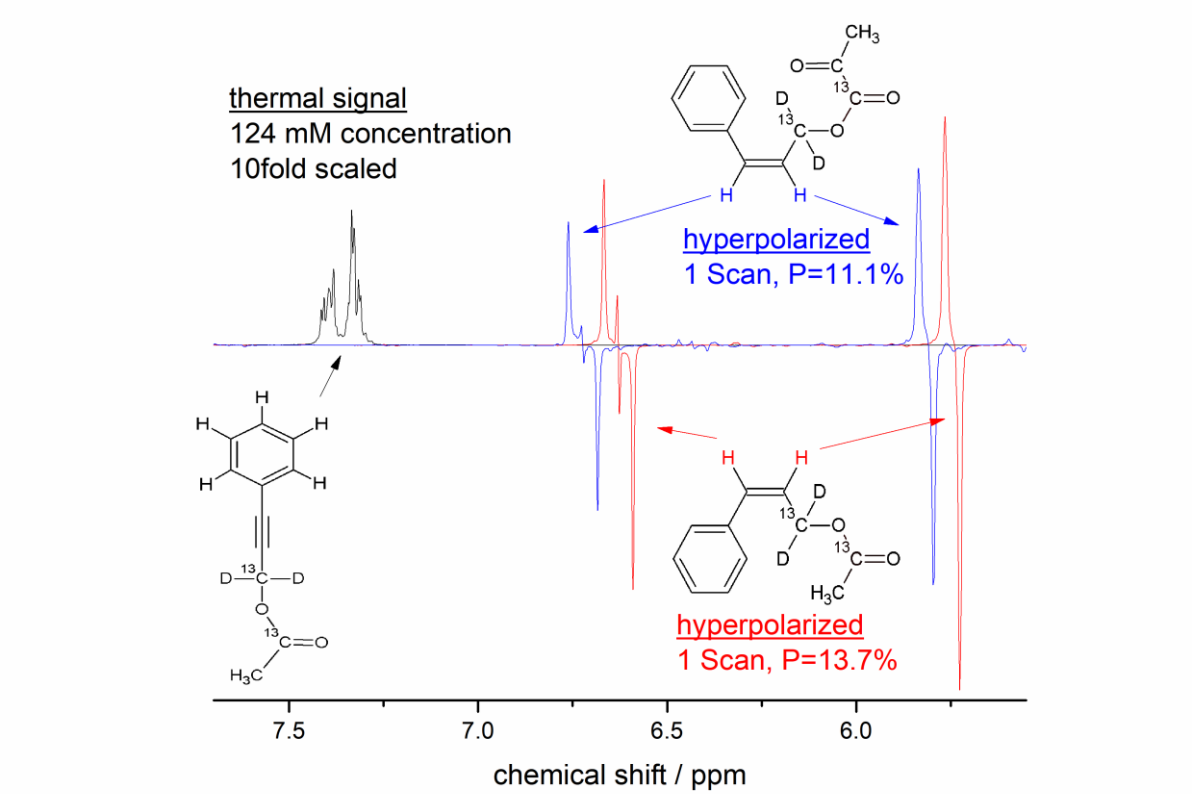

Figure S10. The ^{1}H-NMR spectra in acetone-d_6 of hyperpolarized *cis*-cinnamyl acetate (in red 13.7% polarization) and *cis*-cinnamyl pyruvate (in blue 11.1% polarization) after 20 s para-hydrogenation of 1.5 mM precursor in presence of of the Rh-catalyst are compared to the aromatic part of the spectrum of a 124 mM thermally polarized acetate precursor (in black). The spectra of the hyperpolarized cinnamyl esters were acquired after a 45° flip-pulse. The spectrum of the acetate precursor was acquired after a 90° excitation pulse.

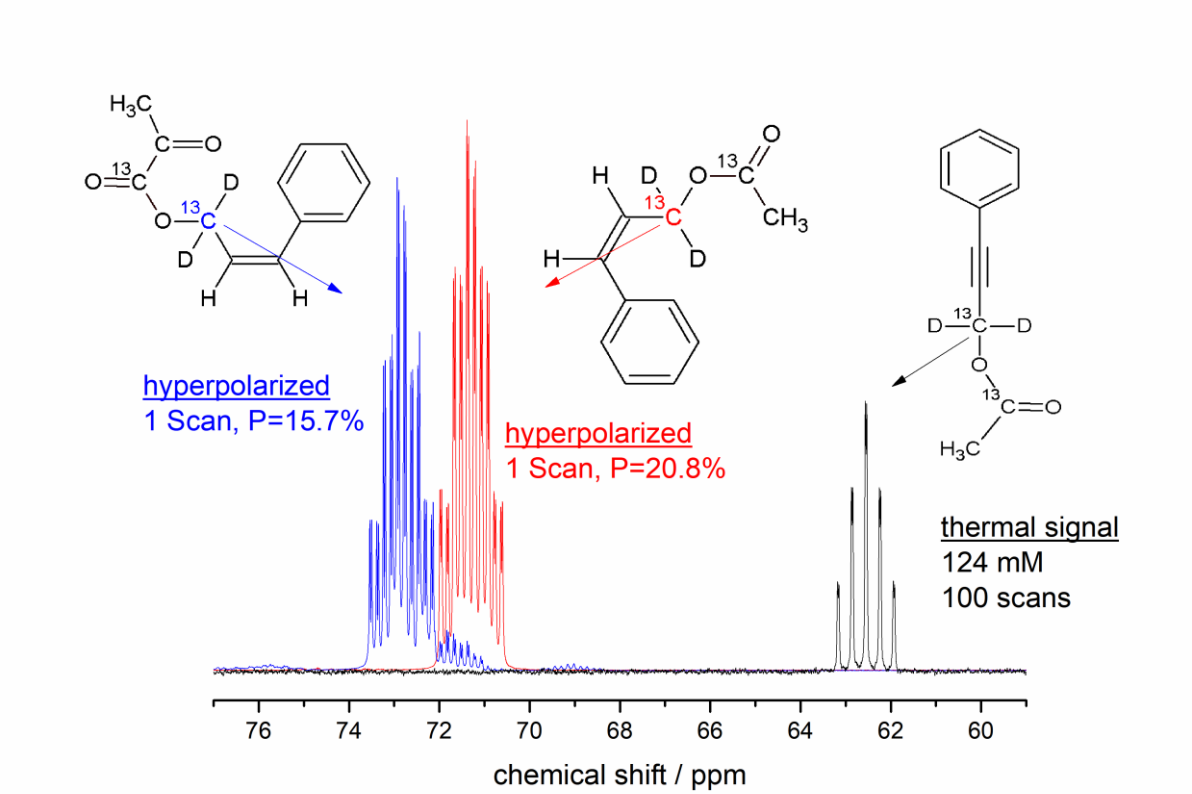

Figure S11. ^{13}C-NMR hyperpolarized spectrum in acetone-d_6 of the cinnamyl acetate and cinnamyl pyruvate after 20 s para-hydrogenation of 1.5 mM precursors in presence of the Rh catalyst and after polarization transfer to the first carbon using the sequence in Figure 2b)-$b_{1)}$, in comparison to the spectrum of a thermally polarized acetate precursor. Polarizations are 20.8% for cinnamyl acetate and 15.7% for cinnamyl pyruvate. The delays were $\Delta_A = \Delta_{C1} = 41.6$ ms, $\Delta_B = 44.6$ ms and $\Delta_A = \Delta_{C1} = 43.4$ ms, $\Delta_B = 41.6$ ms for cinnamyl acetate and for cinnamyl pyruvate, respectively.

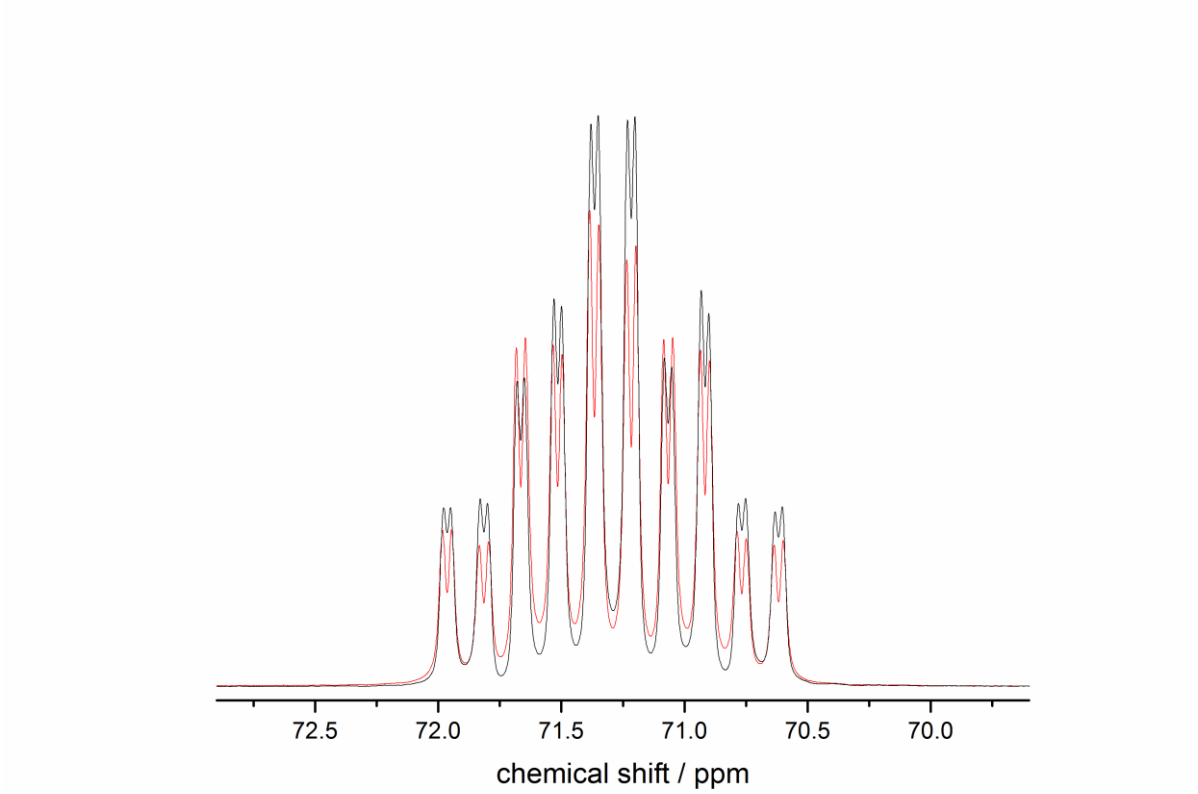

Figure S12. ^{13}C-NMR spectrum in acetone-d_6 of the cinnamyl acetate after polarization transfer to the first carbon using the sequence for transfer to $^{13}C_3$ shown in Figure 3b)-3b$_1$) with selective ^{13}C 180°-pulse (black) and non-selective 180°-pulse (red). The delays were $\Delta_A = \Delta_{C1}$=41.6 ms, Δ_B =44.6 ms.

References:

[1] J. M. Hooker, M. Schönberger, H. Schieferstein, J. S. A. Fowler, *Angew. Chem. Int. Ed.* **2008**, *47*, 5989.

[2] R. R. Schrock, J. A. Osborn, *J. Am. Chem. Soc*. **1976**, *98*, 2143.

[3] A.S. Kiryutin, G. Sauer, S. Hadjiali, A.V. Yurkovskaya, H. Breitzke, G. Buntkowsky, *J. Mag. Reson*. **2017**, *285*, 26.

[4] A. S. Kiryutin, A. N. Pravdivtsev, A. V. Yurkovskaya, H.-M. Vieth, K.L. Ivanov, *J. Phys. Chem. B.* **2016**, *120*, 11978.

[5] O. W. Sørensen, G. W. Eich, M. H. Levitt, G. Bodenhausen, R. R. Ernst, *Prog. Nucl. Magn. Reson. Spectrosc.* **1984**, *16***,** 163.